UNIVERSITIY OF CALIFORNIA SAN DIEGO

Somatic Ultrastructure Enables Precise Predictions of Calcium Signaling Dynamics within Cerebellar Purkinje Neurons

A thesis submitted in partial satisfaction of the requirements
for the degree of Master of Science

in

Biology

by

Yuning Wang

Committee in charge:

Professor Brenda Bloodgood, Chair
Professor Mark Ellisman, Co-Chair
Professor Yishi Jin

2021

The Thesis of Yuning Wang is approved, and it is acceptable in quality and form for publication on microfilm and electronically.

University of California San Diego

2021

DEDICATIONS

I would like to dedicate this thesis to my parents. Their unconditional love and unyielding faith in me have been the solid foundation for me to achieve what I can today and what I yet to tomorrow.

EPIGRAPH

"Look deep into nature, and then you will understand everything better."

Albert Einstein

"… in a scientific pursuit there is continual food for discovery and wonder. …my operations might be incessantly baffled, and at last my work be imperfect, yet when I considered the improvement which every day takes place in science and mechanics, I was encouraged to hope my present attempts would at least lay the foundations of future success."

Mary Shelley, *Frankenstein*

"Every man if he so desires becomes sculptor of his own brain."

Santiago Ramón y Cajal

TABLE OF CONTENTS

Thesis Approval Page iii
Dedications iv
Epigraph v
Table of Contents vi
List of Figures vii
Abbreviations viii
Acknowledgments x
Abstract of the Thesis xii
Introduction 1
Results 10
Discussion 22
Materials and Methods 29
References 33

LIST OF FIGURES

Figure 1. Subcellular organization of a mouse cerebellar Purkinje soma reconstructed via Electron Tomography…….....10

Figure 2. Widespread distributions of Calbindin and PV in cerebellar Purkinje somas ……...….13

Figure 3. PLCβ1 and PLCβ3 distributions in cerebellar Purkinje somas……...……..…16

Figure 4. GPCR distributions in cerebellar Purkinje somas……...…….……19

ABBREVIATIONS

Ca^{2+}	calcium ion
SERCA	sarco/endoplasmic reticulum Ca^{2+}-ATPase
PMCA	plasma membrane Ca^{2+} ATPase
GPCR	G-protein coupled receptor
M3 mAChR	muscarinic acetylcholine receptor M3
mGluR1	muscarinic glutamate receptor 1
5HT2aR	5-hydroxytryptamine (serotonin) receptor 2A
PLCβ1/PLCβ3	phospholipase beta 1/ phospholipase beta 3
IP3	inositol triphosphate
IP3R	inositol triphosphate receptor
TOM20	mitochondrial importer receptor subunit 20
CICR	calcium-induced calcium release
SOCE	store-operated calcium entry
DAG	diacylglycerol
STIM1	stromal interacting molecule 1
CREB	cAMP responsive element binding protein
ERK	extracellular signal regulated kinase
MAPK	mitogen-activated protein kinase
cAMP	cyclic adenosine monophosphate
PKA	protein kinase A
PBS	phosphate buffered saline

ER	endoplasmic reticulum
DAPI	4′,6-diamidino-2-phenylindole
BSA	bovine serum albumin
IHC	immunohistochemistry
PFA	paraformaldehyde
NDS	normal donkey serum
ET	electron tomography
SBEM	serial block-face electron microscopy

ACKNOWLEDGMENTS

I would like to thank all my mentors and friends in Bloodgood Lab and Ellisman Lab that have offered me with opportunities and guided me in my academic path. To Dr. Matthias Haberl, who introduced me to this neuroscience project and therefore forever opened my eyes to real scientific research. He has never ceased to be a very knowledgeable and kind mentor. To Dr. Brenda Bloodgood, who accepted me into her lab and has been super generous with her guidance. I am and will always be honored to have joined her lab and I am very glad to have known a great example of a woman in science. Importantly, I am very thankful for having her as my thesis advisor. To Evan Campbell, who took me under his wing and taught me everything from conducting proper research to how to think critically. I am always in awe of his dedication to science and mentorship. His patient guidance and tireless efforts have helped me expand my horizon and significantly aided me in becoming the researcher I am today. To Ahmed Abushawish, who has been an amazing mentor as well and brought us together in Bloodgood Lab. To Kaitlyn Robinson and Lukas Makrakis, who have been my mates on this research journey. Their friendships and countless supports have made this journey delightful, and I will continue to treasure their companies. Last but not the least, I would like to thank Dr. Mark Ellisman and Dr. Yishi Jin for being on my thesis committee. I will ever feel so privileged and grateful to have them on my committee.

This thesis, in part, is currently being prepared for submission for publication of the material. Co-authors of the publication in preparation include Matthias G. Haberl, Justin Laughlin, Evan P. Campbell, Kaitlyn Robinson, Lukas Makrakis, Andrew Nguyen, Justin Oshiro, Sebastien

Phan, Eric Bushong, Thomas Deerinck, Mark H. Ellisman, Padmini Rangamani and Brenda L Bloodgood. The thesis author was the primary investigator and author of this material.

ABSTRACT OF THE THESIS

Somatic Ultrastructure Enables Precise Predictions of Calcium Signaling Dynamics within Cerebellar Purkinje Neurons

by

Yuning Wang

Master of Science in Biology

University of California San Diego, 2021

Professor Brenda Bloodgood, Chair

Professor Mark Ellisman, Co-Chair

Intracellular calcium (Ca^{2+}) signaling can regulate synaptic plasticity via gene expression in neurons. One pathway that links Ca^{2+} to gene expression is the G-protein coupled receptor - inositol triphosphate receptor (GPCR-IP3R) pathway. Ca^{2+} signaling dynamics could be affected

spatiotemporally by subcellular ultrastructure, such as the endoplasmic reticulum (ER) and distributions of Ca^{2+}-regulating proteins in the GPCR-IP3R pathway. Computational models have been built to better understand intracellular Ca^{2+} signaling but have yet to consider accurate neuronal ultrastructure and protein localizations. In order to make a precise model simulating neuronal Ca^{2+} dynamics, we aimed to analyze realistic somatic ultrastructure and distributions of signaling proteins in the GPCR-IP3R pathway within cerebellar Purkinje neurons. Here, using electron microscopy, we found out that the sub-surface ERs are denser and mostly parallel to the plasma membrane (PM). We performed immunohistochemistry for multiple proteins in the GPCR (coupled to $G_{\alpha q}$ subunit) signaling pathway, but none of these proteins showed prominent asymmetries except for IP3R. In the initial model with idealized geometry, we found out that specific ER membrane structure organization near the PM may facilitate local Ca^{2+} concentration increases. In addition, heterogeneous IP3R distribution could lead to various degrees of Ca^{2+} release from the internal ER Ca^{2+} store. Based on the results above, we concluded that the unique ER organization and heterogeneous Ca^{2+}-signaling protein distributions may shape Ca^{2+} signaling dynamics within the Purkinje somas.

INTRODUCTION

Calcium signaling is ubiquitous and regulates neuronal synaptic plasticity

Calcium (Ca^{2+}) is a ubiquitous signaling molecule that regulates many cellular processes (Berridge et al., 2000). In the brain, the formation of synaptic plasticity which can lead to the formation of memory and learning is regulated by intracellular Ca^{2+} molecules (Apps & Garwicz, 2005; Citri & Malenka, 2008; Nabavi et al., 2014). Associations between Ca^{2+} signaling, synaptic plasticity and the formation of memory and learning were extensively examined. It was reviewed that an altered Ca^{2+} signaling could change the threshold of synaptic plasticity during aging and an association between Ca^{2+} dysregulation and aging-related memory impairment was implicated (Foster & Norris, 1997). Moreover, one study found that an increase in a protein regulated by Ca^{2+}, calcineurin, led to a decline of spatial memory during aging in the rat hippocampus, revealing a link between altered Ca^{2+} signaling and memory deficit (Foster et al., 2001). Overall, Ca^{2+} signaling regulates synaptic plasticity in neurons, which can contribute to memory and learning.

Ca^{2+} signaling regulates synaptic plasticity and eventually the function of memory and learning by acting as a messenger to activate downstream signaling cascades in the cytoplasm or by directly entering the nucleus to initiate neuronal gene transcriptions required to form synaptic plasticity (Berridge, 1998). The Ca^{2+} transient near the nucleus may enter into the nucleus and activate the phosphorylation of a transcription factor called cAMP responsive element binding protein (CREB) in real time after a postsynaptic event; CREB then activates expressions of synaptic adhesion molecules, contributing to synaptic plasticity (Hardingham et al., 1997; Hayer & Bading, 2015; Silva et al., 1998). Besides direct entry into the nucleus, Ca^{2+} can activate the

extracellular signal regulated kinase (ERK) - mitogen-activated protein kinase (MAPK) pathway, which is found to be responsible for long-term synaptic plasticity and memory formation by its signaling into the nucleus (Wiegert & Bading, 2011). In addition, somatic Ca^{2+} transient initiates the cyclic adenosine monophosphate (cAMP) - protein kinase A (PKA) pathway that has implications in neuronal survival and synaptic plasticity (Grewal et al., 2000). Ca^{2+} propagation in the neuronal soma will lead to various subsequent signaling events that can induce gene expression related to synaptic plasticity.

Calcium signaling dynamics may be shaped by neuronal ultrastructure

Intracellular Ca^{2+} propagation is a complex process as it is tightly regulated by many molecules and various compartments in the neurons. One of the regulations of intracellular Ca^{2+} signaling is Ca^{2+} buffers that can bind to Ca^{2+} molecules. Neuronal cytosol is filled with Ca^{2+} buffers such as calbindin and parvalbumin (PV) (Schwaller, 2010). These buffers are readily available to bind to surrounding Ca^{2+} molecules to maintain the somatic Ca^{2+} level very low, which is around 100 nM compared to the extracellular Ca^{2+} level of around 1-2 mM (Gilabert, 2020; Krebs et al., 2015). The reason to maintain this low intracellular Ca^{2+} homeostasis is that Ca^{2+} overload within a cell can lead to excitotoxicity and apoptosis (Orrenius et al., 2003). Most Ca^{2+} transients will be quickly bound to the Ca^{2+} buffers, making it difficult for small Ca^{2+} transients to diffuse further to activate downstream signaling or to induce transcription events (Neher & Augustine, 1992).

Besides cytosolic Ca^{2+} buffers, Ca^{2+} channels at various subcellular membrane structures can also store away or take out the excess Ca^{2+} from the cytoplasm (Berridge et al., 2003). Sarco/endoplasmic reticulum Ca^{2+}-ATPase (SERCA), localized to the endoplasmic reticulum

(ER) membrane, takes Ca^{2+} into the ER store and the intraluminal Ca^{2+} buffer calsequestrin will bind to the Ca^{2+} molecules (Chemaly et al., 2018; Gilabert, 2020). Plasma membrane Ca^{2+} ATPase (PMCA) localized on the plasma membrane (PM) will take excess intracellular Ca^{2+} out into the extracellular space (Calì et al., 2018). Even mitochondria can function as a Ca^{2+} store to remove excess cytosolic Ca^{2+} via the uniporters located on the mitochondrial membrane, although its buffering rate is dependent on the cytosolic Ca^{2+} concentration (Collins et al., 2001). Either cytosolic Ca^{2+} buffers or Ca^{2+} channels located on membrane structures will work to maintain the Ca^{2+} concentration low.

The various types of Ca^{2+} regulation portray a highly dynamic Ca^{2+} signaling. One of the pathways that can lead to a high level of cytosolic Ca^{2+} increase and thus potentially allowing Ca^{2+} to diffuse further is the G-protein coupled receptors - inositol triphosphate receptors (GPCR-IP3R) pathway (Berridge, 1998; W. N. Ross, 2012). After Ca^{2+} fluxes in from extracellular space, local cytosolic Ca^{2+} concentration increases will activate IP3Rs located on the ER. Simultaneously, if a significant neuronal signaling event triggers neurotransmitter release onto the GPCRs located on the PM, GPCRs will be activated (Hagenston & Simonetti, 2014). Activated GPCRs will turn on phospholipase Cβ (PLCβs) via the $G_{\alpha q}$ subunits coupled to the GPCRs to cleave Phosphatidylinositol 4,5-bisphosphate (PIP2) into inositol 1, 4, 5-trisphosphate (IP3) and DAG (Rhee, 2001). IP3, along with local Ca^{2+} increase, activates IP3Rs distributed on the ER membrane, to release Ca^{2+} into the cytosol from the ER internal Ca^{2+} store (W. N. Ross, 2012). As more IP3Rs are activated, Ca^{2+} in the local domain where the activated IP3Rs are is greatly increased (Finch & Augustine, 1998). With the release of the ER internal Ca^{2+} stores, Ca^{2+} could diffuse further, until it is bound by Ca^{2+} buffers (Hartmann & Konnerth, 2005). This Ca^{2+} diffusion has potential

to trigger subsequent signaling cascades, or to enter the nucleus to initiate transcription events given that it is not timely controlled en route (Matthews & Dietrich, 2015).

As previously stated, The ER acts not only as Ca^{2+} stores but also as Ca^{2+} buffering compartments, when cytosolic Ca^{2+} concentration is high and ER Ca^{2+} store is depleted (Blaustein & Golovina, 2001). Since Ca^{2+} is so rapidly controlled, the intracellular organizations of the ER near the PM are crucial determinants of the spatiotemporal distributions of Ca^{2+} molecules (Allbritton et al., 1992; Dickinson et al., 2017; Lock et al., 2019). The ER has been noted to be a continuous and complex network, with many contact points with the PM and other organelles (Terasaki et al., 1994; Y. Wu et al., 2017). A study showed, in the regions of the ER closely associated with the PM, increased accumulations of stromal interacting molecule 1 (STIM1) that senses and controls Ca^{2+} uptake into the ER, in response to Ca^{2+} store depletion (M. M. Wu et al., 2006). Meanwhile, another study observed a decrease of PM-ER contacts after excitatory stimulations in hippocampal CA1 pyramidal neurons (Tao-Cheng & Jung-Hwa, 2018). These two studies showed an association of PM-ER contacts and cellular events, indicating a functional role of PM-ER contacts in mediating intracellular Ca^{2+} signaling. It can be hypothesized that a close PM-ER distance may facilitate Ca^{2+} release from the ER store, because a shorter distance will allow Ca^{2+} to reach the ER in a shorter time, decreasing the chance of most Ca^{2+} to be bound by buffers. Similarly, multiple PM-ER contacts may also facilitate the Ca^{2+} release from the ER store by increasing the chance of Ca^{2+} reaching IP3Rs before being bound.

Since IP3Rs are localized on the ER, the density and the exact location of IP3R might affect Ca^{2+} propagation spatiotemporally. Regenerative Ca^{2+} release is an example of a prolonged and larger cytosolic Ca^{2+} increase due to close proximity of IP3Rs (Bootman et al., 1997; Lock et al., 2019). When both Ca^{2+} and IP3 bind to IP3Rs, a great number of Ca^{2+} molecules are released from

ER stores. When local IP3 concentration is high, released Ca^{2+} will be able to activate other IP3Rs in the vicinity of the activated IP3Rs, as far as IP3 is present (W. N. Ross, 2012). The characteristic of regenerative Ca^{2+} release suggests that the degree of the regenerative release has to do with the quantity of IP3Rs in the vicinity or the spacings between IP3Rs, as clusters of IP3Rs in the vicinity or small spacings will allow more IP3Rs to be activated, releasing more Ca^{2+} (Swillens et al., 1999; Taylor et al., 2009). As it turns out, small clusters of IP3Rs near the PM initiate almost all Ca^{2+} puffs (by regenerative Ca^{2+} release), indicating the importance of IP3R density and distribution in facilitating Ca^{2+} signaling (Thillaiappan et al., 2017). Furthermore, it has been shown that IP3Rs were concentrated at close membrane appositions including ER inner stacks and ER cisternae next to the PM, while regions further away from the membrane appositions see less IP3Rs (Satoh et al., 1990; Takei et al., 1992). Therefore, it can be hypothesized that IP3Rs have unique distributions that can influence Ca^{2+} propagation.

Distributions of other Ca^{2+}-signaling proteins in the GPCR-IP3R pathway may as well influence Ca^{2+} signaling dynamics. As the initiators of this pathway, GPCRs activate PLCβs to produce IP3 at the PM site (Dhyani et al., 2020). The initiation and direction of IP3 diffusion will likely influence where and how many IP3Rs are activated, based on the regenerative Ca^{2+} release described above. Therefore, it is hypothesized that the localizations of both GPCRs and PLCβs may influence Ca^{2+} signaling dynamics.

Existing models of intracellular calcium diffusion

To decipher intracellular Ca^{2+} signaling dynamics, computational models were successfully built to simulate Ca^{2+} diffusion in different intracellular conditions. For example, in order to understand how neural activity may influence intracellular Ca^{2+} signaling dynamics spatiotemporally in astrocytes, a model was constructed based on Ca^{2+} concentrations in different

subcellular compartments and rate of Ca^{2+} uptakes and Ca^{2+} diffusion coefficients (Cresswell-clay et al., 2018). This study has yielded significant results showing that neural activity is important in deciding the rate of Ca^{2+} waves, but the study simplified the distributions of subcellular compartments and assumed all compartments have the same volume and surface. In another model investigating Ca^{2+} waves initiated by IP3Rs in neuroblastoma cells, distributions of ERs were considered as the foundation of the model; however, although the ER distribution densities are different across different neuronal domains such as the dendrite and the soma, but the ER density within the neuronal soma is considered homogeneous (Fink et al., 2000). Clearly, to simplify the computational process, current models studying Ca^{2+} signaling dynamics did not consider more realistic and finer subcellular ultrastructure and its precise impact on Ca^{2+} signaling dynamics.

Because of the limitation of existing models to accurately reflect the Ca^{2+} dynamics within realistic cellular environment, these models have not showed how subcellular organization may influence Ca^{2+} dynamics in depth. To gain more insights into how ultrastructure may shape Ca^{2+} signaling dynamics, we are interested in constructing a model of Ca^{2+} diffusion based on analysis of realistic neuronal ultrastructure. Our model in vision may provide clues of the spatiotemporal effects of subcellular ultrastructure on Ca^{2+} dynamics.

Proposed model of calcium diffusion in cerebellar Purkinje somas

Based on the hypothesis that subcellular ultrastructure and important Ca^{2+}-signaling protein distributions may influence Ca^{2+} signaling dynamics, we propose a Ca^{2+} diffusion model based on realistic ultrastructure and Ca^{2+}-signaling proteins in the Purkinje somas.

We chose Purkinje neurons to be the ideal place to model somatic Ca^{2+} signaling dynamics. The reasons that we choose cerebellar Purkinje neurons are that they have large cell bodies, a

variety and high concentrations of signaling molecules and buffers and also elaborate ER networks within (Gruol et al., 2012). Although Ca^{2+} signaling dynamics within the Purkinje dendritic spines has been thoroughly examined, the dynamics within the somas has not been studied before (Bloodgood & Sabatini, 2007). The large somatic space of the Purkinje neuron makes Ca^{2+} diffusion highly dynamic and complex due to the presence of multitudes of Ca^{2+} buffers such as calsequestrin, calbindin, PV that make up the intricate environment for Ca^{2+} signaling (Empson & Knöpfel, 2012; Fierro & Llano, 1996; Hartmann & Konnerth, 2005). In addition, cerebellar Purkinje neurons have been the focus to study Ca^{2+} signaling in because they are well associated with synaptic plasticity and contribute to motor learning controlled by the cerebellum (Hartmann & Konnerth, 2005; Hoxha et al., 2016; Ito, 2002). One study has shown that mice with knock-out PCP4 gene, responsible for regulating calmodulin-dependent synaptic plasticity, showed altered long-term depression at Purkinje synapses (Wei et al., 2011). These knockout mice also demonstrated deficits at learning locomotor tasks, indicating the importance of cerebellar Purkinje neurons at regulating motor learning. Therefore, we choose to focus our model on the Ca^{2+} signaling dynamics within the cerebellar Purkinje neurons.

To build this model of simulated calcium diffusion, Ellisman Lab, Rangamani Lab and Bloodgood Lab at UCSD joined forces and each completed one of three aspects of modeling. Ellisman Lab provided 3D reconstructions of Purkinje somatic ultrastructure based on electron tomography (ET) and serial block-face electron microscopy (SBEM) datasets of Purkinje neurons. Structural arrangements of ERs, mitochondria, PMs and golgi apparatus were analyzed based on the 3D reconstructions and to be used as realistic structural inputs into the model. Rangamani Lab focused on building the model based on previous experimental data of Ca^{2+} and IP3 diffusion and Ca^{2+} buffering. The model used partial differential equations (PDEs) that can provide

spatiotemporal dynamics in response to a postsynaptic event. With experimental parameters and PDEs, an initial model with idealized geometry of ultrastructure was built; idealized Ca^{2+} diffusion was tested with different PM-ER distance, ER orientation and inner ER distance. Later, a model with realistic ultrastructural parameters will be constructed and compared to the idealized model. To see whether spatial distributions of Ca^{2+}-regulating proteins are heterogeneous and whether the heterogeneity helps define Ca^{2+} signaling dynamics, Bloodgood Lab stained for various proteins in cerebellar Purkinje neurons via immunohistostaining (IHC), including calbindin, PV, IP3R, RyR, mGluR1, 5HTaR, M3 mAChR, PLCβ1, PLCβ3, PMCA, SERCA, CLIMP63 and TOM20. Distributions of the protein fluorescence were analyzed; proteins with heterogeneity will be input into the realistic model.

In this thesis, I will focus on the importance of the somatic ultrastructure near the PM on Ca^{2+} signaling dynamics within the Purkinje somas. This region near the PM is of particular interest to me because Ca^{2+} signaling is initiated in this subcellular region and the organization of ERs and Ca^{2+}- regulating proteins may play a huge part in further Ca^{2+} propagation. First, spatial organizations of sub-surface ERs will be analyzed based on ET images and analysis. To bridge the ET analysis and the IHC analysis, Calbindin and PV as widely distributed proteins, PMCA as plasma membrane protein and TOM20 as a mitochondrial membrane protein were analyzed to confirm their expected distribution patterns. Then the distributions of Ca^{2+}-signaling proteins including PLCβ1 and PLCβ3 will be discussed in detail, while IP3R and RyR will be briefly discussed based on analysis done by other collaborators. Last but not the least, we chose M3 mAChR and 5HT2aR as alternatives of mGluR1, the default GPCR in our model, to see if they have significant distribution patterns and also be considered in the model. mGluR1 was initially chosen because the synaptic input of the model was based on a glutamate release event. M3

mAChR was selected because this isoform couples to $G_{\alpha q}$ subunit to stimulate PLC activation and has been shown to lead to cytosolic Ca^{2+} increase that propagates from apical dendrite to soma in hippocampus (Caulfield, 1993; Kruse et al., 2012; Power & Sah, 2002). Similarly, 5HT2aR was selected as possible alternative to mGluR1 since 5HT2aR has been shown to increase Ca^{2+} availability in neurons (Azmitia, 2001). Overall, by analyzing subcellular ultrastructure and protein distributions, we should be able to see the spatiotemporal influence the Purkinje somatic ultrastructure may have on Ca^{2+} signaling dynamics, providing insights into the importance of accurate modeling of Ca^{2+} diffusion.

Organization of the subcellular ER

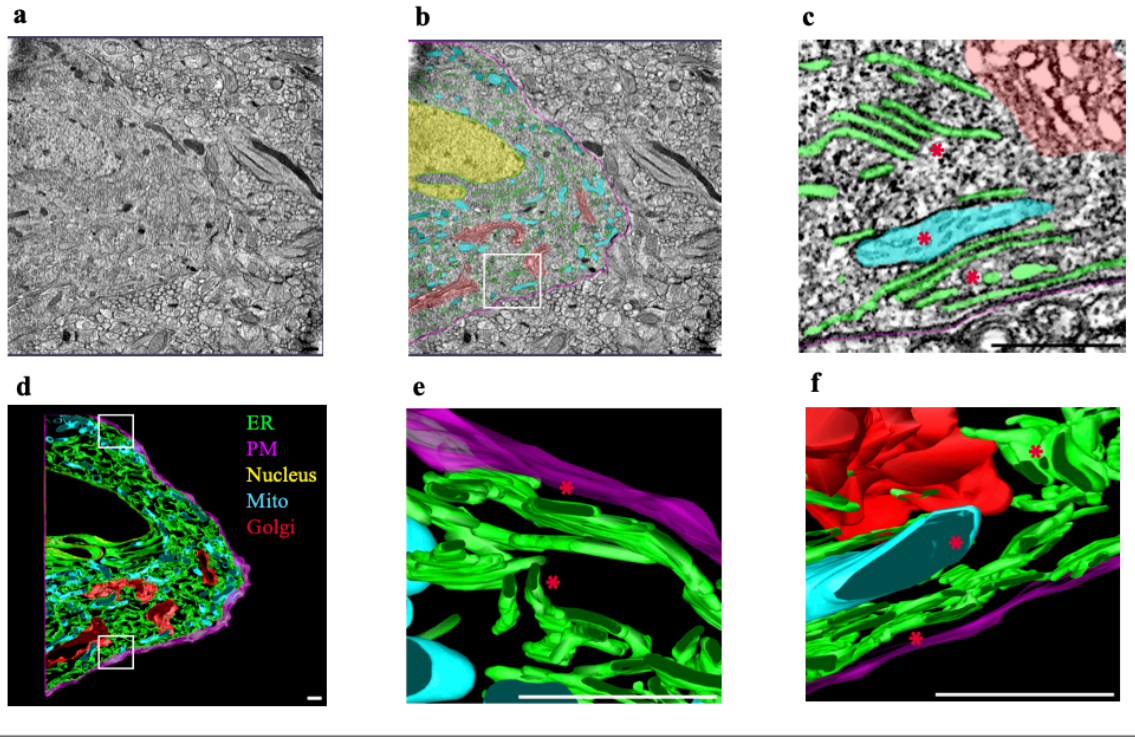

Figure 1. Subcellular organization of a mouse cerebellar Purkinje soma, reconstructed via Electron Tomography. (**a, b**). A single plane of a volumetric electron tomogram (ET) (z = 73) based on a mouse cerebellar tissue section shows a partial Purkinje soma. Resolution is 12 x 12 x 0.44 μm^3. (b) shows 2D annotations of subcellular structures based on the single plane ET, (a). Subcellular structures were identified and annotated: ER (green), mitochondria (cyan), plasma membrane (magenta), golgi apparatus (red) and nuclear membrane (yellow). To closely see the intracellular membrane ultrastructrure near the PM, the white box area was examined in (c). (**c**). 2D annotations showing sub-surface ERs and mitochondrias. The top red asterisk marks ERs that are non-parallel to the PM. The middle asterisk marks a mitochondrium a distance away from the PM. The bottom asterisk marks sub-surface ERs. (**d**). Purkinje subcellular structures of the whole volumetric ET dataset were 3D reconstructed. To closely see intracellular organizations near the PM, the top white box area was closely examined in (e) while the bottom white box area in (f). (**e, f**). 3D reconstructions focusing on two regions of sub-surface ERs. In (e), top red asterisk marks sub-surface ERs, while bottom asterisk marks non-parallel ERs furtherer away from the PM. In (f), the left bottom asterisk marks sub-surface ERs. The middle asterisk marks a mitochondrium that is a distance away from the PM. The top right asterisk marks non-parallel ERs further away from the PM. Scale bars = 600 nm.

To reconstruct the somatic space of the cerebellar Purkinje neurons, volumetric electron tomography (ET) and serial-block scanning electron microscopy (SBEM) were performed on mouse cerebellar tissues to reveal the Purkinje structural organizations in high resolution. Structures such as the ER, the PM, the mitochondria, the golgi apparatus and the nuclear membrane

were segmented first by the deep learning image segmentation tool CDeep3M and then manually annotated and corrected (Fig. 1a, 1b) (Haberl et al., 2018). The datasets were then 3D reconstructed to show the spatial occupancies of subcellular structures in the somatic space (Fig. 1d).

The whole somatic space of the Purkinje soma is tightly occupied by various organelles; the ER especially occupies a large space and can be seen as an intricate network throughout the whole neuronal soma section (Fig. 1a, 1b, 1d). This subcellular organization is very different from the ideal schematic of the cellular space with only a few stacks of ER that biology textbooks have shown. The tight intricate network of the ER is further supported by the analysis of ER occupancy within the somatic space, in 93.44% of which the ER can be found within 250 nm (Haberl et al., in preparation).

Upon closer examination of the distribution of the ER, it is evident that the ER distributes very close to the PM and have different orientations to the PM (Fig. 1c, 1e, 1f). Radial distribution of the somatic membrane structures shows that the ER has a denser volume fraction (about 16%) in the subsurface region (0-100 nm from the PM) of the somatic space, whereas the mitochondria have a denser population further away from the PM (200 nm and further from the PM) (Haberl et al., in preparation). As for the orientation of the ER to the PM, the ER can be oriented from 0 to 180 degrees to the PM, although most are found parallel to the PM, meaning they are either at either 0 degree or 180 degrees (Fig. 1c, 1e, 1f). It is further shown that as the PM-ER distance is small, the ER is mostly parallel to the PM. The sub-surface ER tend to be mostly parallel to the PM (Fig. 1c, 1e, 1f; Haberl et al., in preparation).

EM reconstructions show that the ER has a high occupancy near the PM, and it is found to be mostly parallel in the sub-surface region. To understand if this specific organization has any influence on the calcium signaling dynamics near the PM, Ca^{2+} diffusion was simulated in a model

with idealized geometry, where different PM-ER distances and ER orientations were tested (Haberl et al., in preparation). After Ca^{2+} entry into the cytosol, more Ca^{2+} will be released from the ER store if the PM-ER distance is shorter or if the ER is parallel or almost parallel to the PM. Moreover, the Ca^{2+} concentration in the ER stacks will reach a higher peak at an earlier time (~120 ms) if the ER is parallel to the PM, compared to the times taken to see a peak Ca^{2+} concentration where the ER is perpendicular (~130 ms) or at a 45-degree angle to the PM (~140 ms). These above results indicate that the sub-surface ER may facilitate Ca^{2+} diffusion.

In the above calcium diffusion model with idealized geometry, the distributions of calcium-releasing proteins such as IP3Rs or RyRs are randomly distributed on the ER membrane structure (Haberl et al., in preparation). However, the simulated calcium dynamics might not portray an accurate intracellular calcium signaling environment, if the calcium-regulating proteins are not randomly distributed. Therefore, in the below sections, we aim to investigate whether proteins that participate in the GPCR-IP3R signaling pathway have any distribution patterns that may potentially influence the calcium dynamics that we observed in the model with idealized geometry.

Detections of both wide and highly polarized protein distributions via IHC analysis

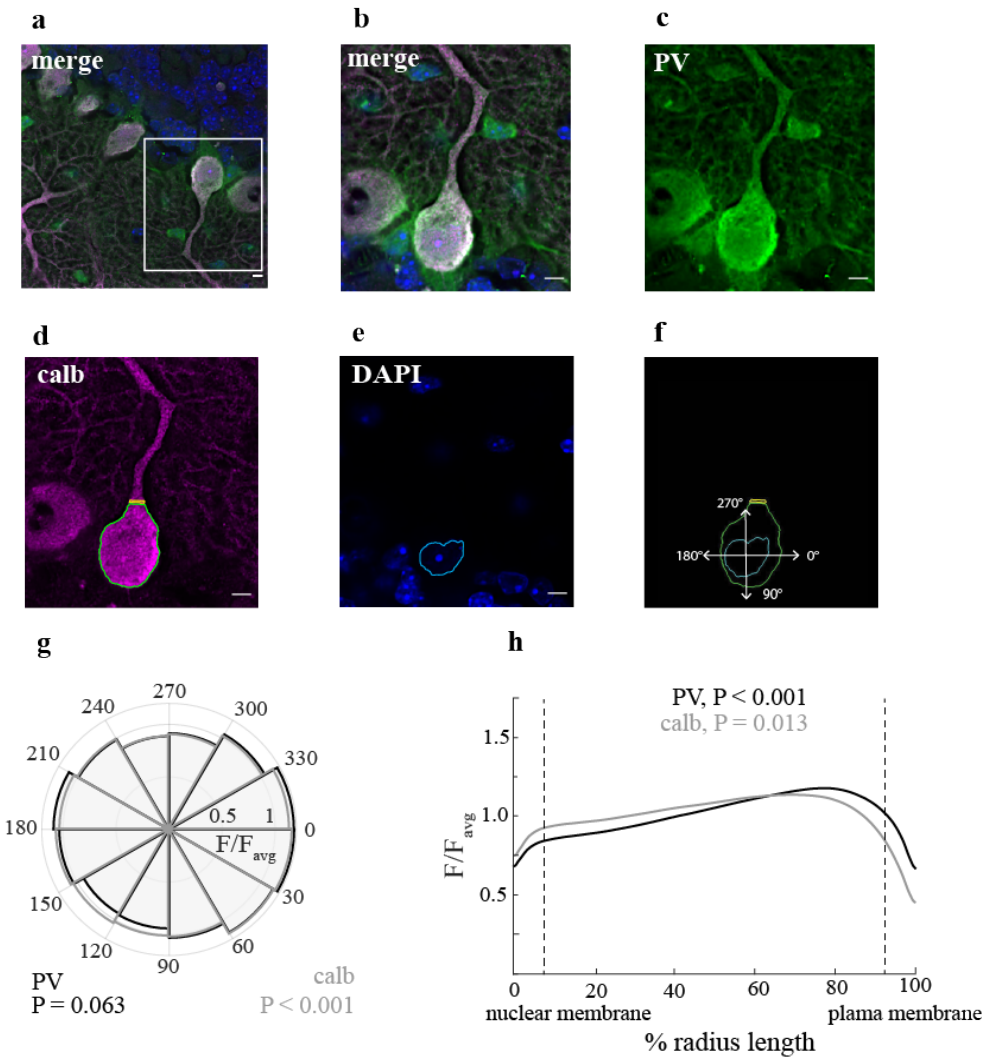

Figure 2. Widespread distributions of calbindin and PV in cerebellar Purkinje somas. (**a**). a single plane of a multi-plane confocal image displaying immunofluoresences of calbindin (calb), parvalbumin (PV) and DAPI, in mouse cerebellar molecular and granular layers. White box area is zoomed in in (b). scale bar = 5 μ m. (**b** - **e**). a view of merged fluorescence (b) , PV fluorescence (c), calb (d) and DAPI (e) centered on a single Purkinje neuron. The yellow and the green tracings (d) show masks for a small section of apical dendrite connecting to soma and the soma body, respectively. Apical dendrite and soma is divided based on cell curvature. The blue tracing (e) shows a mask for the nucleus. scale bar = 5 μm (in b-e). (**f**). a combination of apical dendrite, soma and nucleus masks. The masks are used in analysis to cover regions of interest only. The polar coordinate shows how the cell is centered and segmented in analysis. (**g**). shows an angular analysis of the average PV and calb fluorescences across eighteen neurons. The radius axis of the analysis represents PV (black) or calb (gray) fluorescence intensity (F) over the average fluorescence intensity (F_{avg}). Each bin represents the F/F_{avg} over a 30 degree sector of the Purkinje cytosol. ($p_{PV} = 0.0631$, $p_{calb} = 0.0002$). (**h**). shows a radial analysis of the average PV and calb fluorescences across eighteen neurons. F/F_{avg} was analyzed from nuclear membrane boundary to plasma membrane boundary, in average percent radius length. Dotted lines are one resolution length from the nuclear membrane and plasma membrane masks and indicate where on average the membranes are due to a resolution limit.

Before we look into whether the proteins in the GPCR-IP3R signaling pathway have any distribution patterns that could influence the Ca^{2+} dynamics near the PM, we looked into the Ca^{2+} buffers PV and calbindin to see if we can detect wide distribution pattern, since these two proteins have been known to be highly and uniformly expressed within the Purkinje somas (Fig. 2a - 2e). After constructing boundary masks for both nuclear membranes and PMs, we set the region for fluorescence intensity analysis to be within the Purkinje cytoplasm exactly (Fig. 2d - 2f). Within the cytoplasm, PV and calbindin fluorescence intensities over the total average fluorescence intensity (F / F_{avg}) were analyzed angularly in 30-degree sub-regions around the whole soma (Fig. 2g) and radially from the nuclear membrane boundary to the PM boundary (Fig. 2h).

Angular and radial analyses show that PV and calbindin are both widely distributed within the Purkinje somas (Fig. 2g, 2h). A slightly lower distribution in the 240- to 270- degree sections of the soma was observed for PV, but the overall distribution was not significant ($p = 0.063$). The same fluorescence bias was observed for calbindin as well. Nonetheless, we found a significant angular distribution for calbindin ($p < 0.001$) (Fig. 2g). This differences in the P-values yet the same trend could be explained by the different variances of fluorescence in the PV and calbindin fluorescence, as PV fluorescence has a higher variance and therefore an insignificant angular distribution. Looking at the radial fluorescence distributions, a preference towards the PM was observed for both PV ($p < 0.001$) and calbindin ($p = 0.013$), as small increases in F / F_{avg} was seen from the nuclear membrane boundary to the PM boundary. The above slight decrease of fluorescence in the 240- to 270-degree sections and towards the PM were also noticed in the calbindin analysis in Haberl et al., in preparation (angular $p = 0.0717$, radial $p = 0.023$).

To see if we can detect highly polarized proteins, PMCA staining was analyzed (Haberl et al., in preparation). In the confocal images, PMCA could be seen as prominently localized to the PM. It is found that PMCA has a high radial preference towards the PM ($p<0.0001$), which is distinctly different than the wide distribution observed for calbindin and PV. To bridge the structural analysis of ET and distribution analysis of IHC, mitochondria importer receptor subunit 20 (TOM20) located on mitochondria was stained and analyzed (Haberl et al., in preparation). In the IHC analysis, mitochondria preferentially localize towards the apical dendrite in the angular analysis ($p = 0.0042$) and towards the nuclear membrane ($p < 0.0001$). The radial observation of TOM20 seems to overlap with the radial density observation based on 3D reconstructions that the mitochondria have a higher density away from the PM (Haberl et al., in preparation).

Distributions of PLCβs in the Purkinje somas

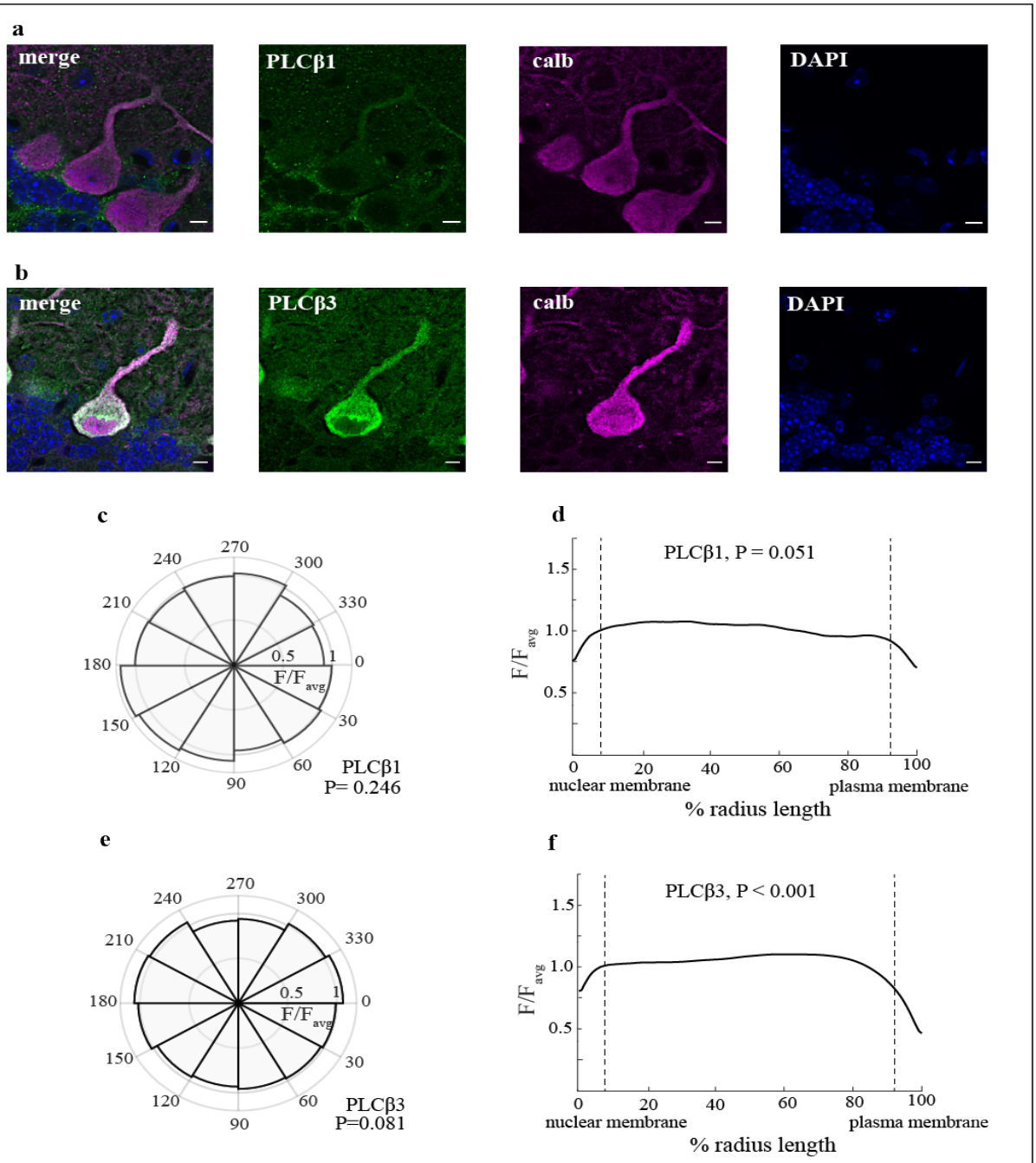

Figure 3. PLCβ1 and PLCβ3 distributions in cerebellar Purkinje somas. (**a** - **b**). confocal images centered on a single mouse cerebellar Purkinje neuron, displaying merged fluorescence, PLCβ1 (a) / PLCβ3 (b) fluorescence, calb fluorescence and DAPI fluorescence, respectively. Scale bars = 5 μm. (**c, e**). angular analyses of the F/F_{avg} of PLCβ1 (c) and PLCβ3 (e) in Purkinje cytosols (n = 18) that were segmented into 30-degree sectors. The radius axis represents F/F_{avg}. PLCβ1, p = 0.246; PLCβ3, p = 0.081. (**d, f**). radial analyses of the F/F_{avg} of PLCβ1 (d) and PLCβ3 (f) in Purkinje cytosols (n =18). The analysis was performed along the radius (measured as % radius length) of the Purkinje cytosols, from the nuclear membrane boundary to plasma membrane boundary. Dotted lines are one resolution length from the masks of plasma membrane and nuclear membrane. PLCβ1, p = 0.051; PLCβ3, p < 0.001.

After confirming the detections of two very different distribution patterns (one is wide distribution and one is highly polarization to the PM), we tested if any significant distribution patterns can be observed for proteins involved in the GPCR-IP3R signaling pathway near the PM. In the GPCR-IP3R pathway, PLCβ, upon activation by the $G_{\alpha q}$ subunit coupled to GPCRs, cleaves the membrane phospholipid PIP2 into DAG and IP3 (Kadamur & Ross, 2013). Since PLCβ is closely associated with the $G_{\alpha q}$ subunit and its substrate PIP2, it is expected to be localized right beneath the PM. To determine their distribution patterns, angular and radial analyses of PLCβ1 and PLCβ3 were performed as previously discussed.

The overall somatic PLCβ1 expression is not strong, although slightly higher expression could be observed near the basal pinceau region of the Purkinje neuron and in the apical dendrite (Fig. 3a). This small preference towards the basal PM can be seen in the angular distribution analysis as well, as demonstrated by the higher F / F_{avg} from 90- to 180- degree sub-regions (Fig. 3c). Albeit the basal PM preference, PLCβ1 does not have a significant angular distribution pattern across the Purkinje somatic space ($p = 0.246$). Except for the slight basal PM preference, not much PLCβ1 distribution could be detected near or beneath the whole PM. This observation is further confirmed by the radial analysis where the F / F_{avg} stayed relatively the same near the PM boundary or along the whole average radius from the nuclear membrane to the PM ($p = 0.051$) (Fig. 3a, 3d). Based on the above data, PLCβ1 does not seem to be highly expressed within the Purkinje soma.

In contrast to PLCβ1, PLCβ3 is highly expressed in the somatic space (Fig. 3b). The angular distribution of PLCβ3 is not significant ($p = 0.081$) (Fig. 3e). However, radial PLCβ3 distribution is significant, as the F / F_{avg} drops off near the PM boundary, indicating a bias away from the PM ($p < 0.001$) (Fig. 3f). This bias does not correlate to the expectation that PLCβ3 is

most active at the PM site, and further testing will be considered, Overall, PLCβ1 is not highly expressed within the soma while PLCβ3 has a widespread distribution.

Distributions of IP3Rs within the Purkinje somas

After analyzing the somatic distributions of GPCR-IP3R pathway proteins PLCβ1 and PLCβ3, we could not find any significant asymmetric distribution patterns. Besides the PLCβs, IP3R also participates in the GPCR-IP3R pathway and is an important calcium-releasing protein to consider in the calcium diffusion model. IP3R is mainly stained and analyzed by collaborators Kaitlyn Robinson and Evan Campbell. They discovered that although IP3R has a non-significant angular distribution overall ($p = 0.0569$), a decrease of F / F_{avg} near the apical pole of the Purkinje soma can be observed as the regions spanning 240-300 degrees have significantly less IP3R than other sub-regions (Haberl et al., in preparation).

Moreover, in the radial analysis, a preference towards the PM was found ($p = 0.0083$). Based on these findings, IP3R does have am asymmetric distribution pattern and its influence on the Ca^{2+} dynamics near the PM should be further investigated in a realistic calcium diffusion model.

Distributions of GPCRs in the Purkinje somas

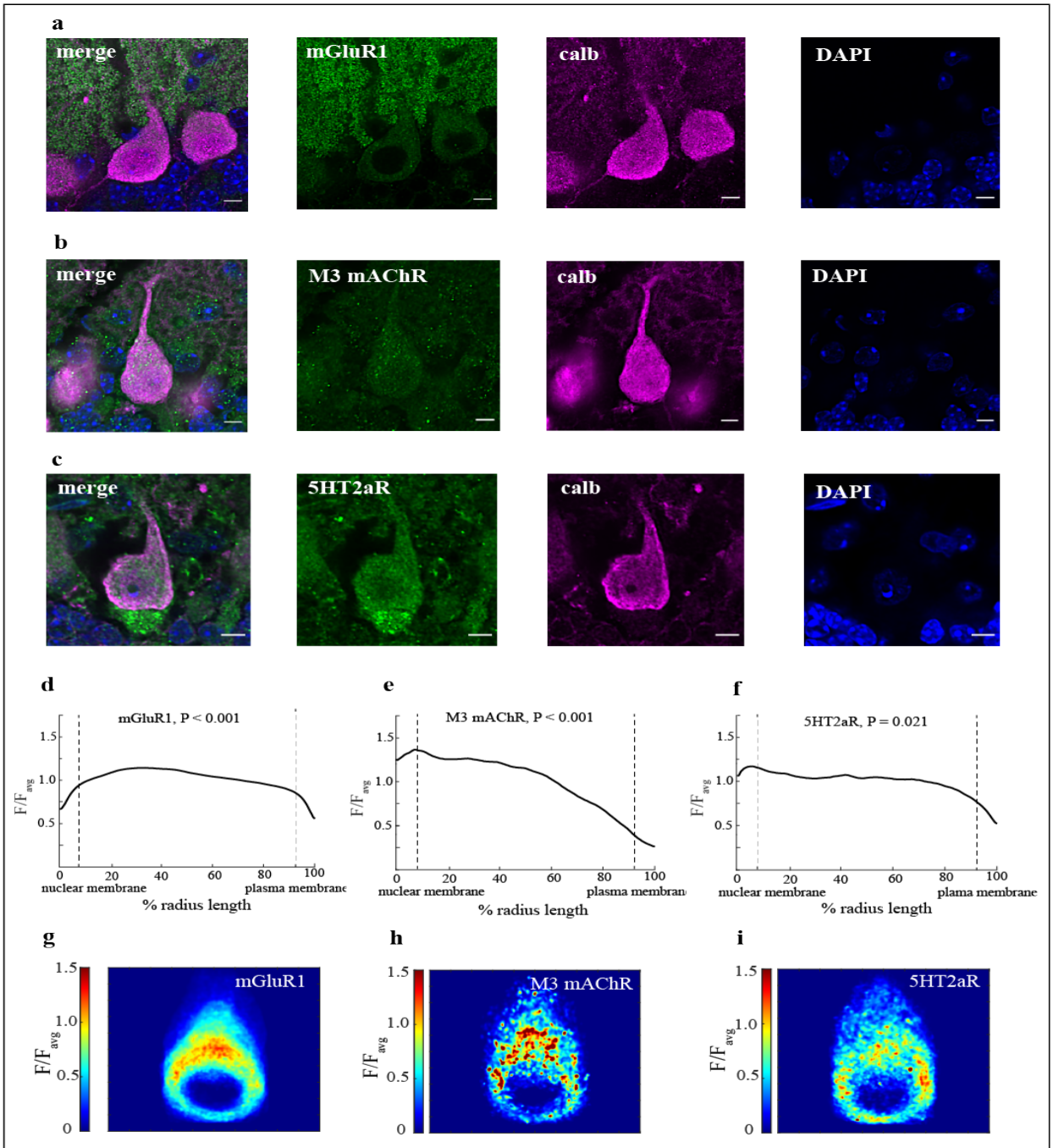

Figure 4. GPCR distributions in cerebellar Purkinje somas. (**a** - **c**). confocal images centered on a single mouse cerebellar Purkinje neuron, displaying merged fluorescence, mGluR1 (a) / M3 mAChR (b) / 5HT2aR (c) fluorescence, calb fluorescence and DAPI fluorescence, respectively. Scale bars = 5 μm. (**d** - **f**). radial analyses of the F/F_{avg} of mGluR1 (d), M3 mAChR (e) and 5HT2aR (f) in Purkinje cytosols (n =18). The analysis was performed along the radius (measured as % radius length) of the Purkinje cytosols, from the nuclear membrane boundary to plasma membrane boundary. Dotted lines are one resolution length from the masks of plasma membrane and nuclear membrane.. mGluR1, $p < 0.0001$; M3 mAChR, $p < 0.0001$; 5HT2aR, $p = 0.0208$. (**g**-**i**). heatmaps of F/F_{avg} of mGluR1 (g), M3 mAChR (h) and 5HT2aR (i) in Purkinje cytosol spaces. The colorbars on the left represent the scale of $F/F_{avg.}$

GPCRs are important proteins to consider in our calcium diffusion model since the activation of GPCRs begin the GPCR-IP3R pathway, allowing Ca^{2+} to propagate further. mGluR1 was integrated in the calcium diffusion model because the main input into the model consists of a glutamate pulse and it was initially randomly distributed in the idealized model. To see whether mGluR1 is heterogeneously distributed on the PM, its distribution in the Purkinje somatic space was examined.

mGluR1 does not appear to have a strong presence within the somatic space, though it can be clearly detected in the Purkinje dendritic spines (Fig. 4a). As for the fluorescence within the somatic space, if it is localized to the PM, mGluR1 fluorescence trend should be similar to the trend of PMCA, which was observed to be significantly polarized to the PM (Haberl et al., in preparation). However, such a strong localization to the PM could not be observed for mGluR1. Its presence, especially on the PM, is very weak and only traces of marginally brighter fluorescence could be observed along the PM boundary. The weak presence of mGluR1 on the PM was not expected as mGluR1 should be predominantly active on the PM as a transmembrane protein. The weakly detected somatic fluorescence on the PM in the confocal images is supported by the radial distribution, as reduced F / F_{avg} was seen near the PM boundary ($p < 0.001$) (Fig. 4d). Additionally, the heatmap of mGluR1 distribution in the somatic space agrees with the radial distribution that mGluR1 seems to have a slightly reduced expression near the PM (Fig. 4g). However, since the staining of GPCRs were done with permeabilization that allows any internal mGluR1 to be stained as well, the confocal images could not provide straightforward evidence whether mGluR1 has a distribution pattern on the PM. Therefore, little conclusion could be made from the mGluR1 analyses.

Besides mGluR1, there are other GPCRs that can contribute to the GPCR-IP3R pathway. Next examined were the somatic distributions of M3 mAChR and 5HT2aR, to see if any significant distribution patterns could be observed. Neither M3 mAChR nor 5HT2aR has strong expression within the Purkinje somas that can be easily detected as calbindin staining for the same neuron (Fig. 4b, 4c). The radial analyses show significant F / F_{avg} decreases near the PM boundary for both proteins (Fig. 4e, 4f). In addition, heatmaps could also provide visual confirmations of the weak presence of fluorescence at the PM compared to the cytosol (Fig. 4h, 4i). As mentioned previously, GPCR immunostaining was done with permeabilization, making it more difficult to identify and isolate the protein fluorescence at the PM. Therefore, little conclusions can be drawn about the distribution patterns for 5HT2aR and M3 mAChR.

DISCUSSION

Our findings provided supporting evidence that somatic ER ultrastructure may shape the local Ca^{2+} dynamics spatially and temporally in an idealized Ca^{2+} diffusion model. The ER is a very important intracellular organelle that regulates Ca^{2+} by acting as both a Ca^{2+} store and a Ca^{2+} release mechanism (Berridge, 1998). In the cytosol space, the ER was found to be a continuous membrane structure from the nucleus to the plasma membrane, forming an intricate network with various structural motifs (Nixon-Abell et al., 2016). Based on our 3D reconstructions of the ET and SBEM datasets, we were able to confirm the complexity and large occupancy of the ER structure as the ER occupies the entire somatic space and forms an elaborate network throughout the Purkinje neuron (Fig. 1, Haberl et al., in preparation). Upon close inspection, the ER has the highest density and is mostly parallel near the PM (Haberl et al., in preparation). These findings are supported by Wu et al. 2017 that the PM-ER contact in the cell bodies is very high (12.48% of the PM) with large ER cisternae closely apposed to the PM. To see whether this close PM-ER apposition and parallel orientation of ER have any influence on intracellular Ca^{2+} dynamics, different PM-ER distances and ER orientations to the PM were tested in the calcium diffusion model with idealized geometry. In the model, parallel orientation of the ER resulted in the earliest (at 120 ms) Ca^{2+} gradient increase and both parallel orientation of the ER and smaller PM-ER distance resulted in more Ca^{2+} molecules released from the ER internal Ca^{2+} store (Haberl et al., in preparation). Possible explanations for the above results could be that a greater number of ER-PM contacts could be formed if the PM-ER distance is small or if the ER strand is parallel to the PM. A greater number of PM-ER contacts may suggest a timely regulation of local intracellular Ca^{2+}, which is important for Ca^{2+}-signaling dynamics (Stefan et al., 2013). Indeed, PM-ER contacts are important for store-operated Ca^{2+} entry (SOCE), which recruits the help of STIM1

protein located on the ER and calcium release-activated calcium channel protein 1 (Orai1) on the PM to replenish Ca^{2+} store, after ER Ca^{2+} store is depleted (Moccia et al., 2015).

We were able to detect both widely distributed and highly polarized proteins, based on the analyses of PV, calbindin and PMCA. PV and calbindin as Ca^{2+} buffers were expected to be highly and uniformly distributed (Maskey et al., 2010; Talamoni et al., 1993). In our IHC experiments, calbindin and PV are highly expressed and widely distributed within the whole somatic space (Fig. 2, 3a, 3b, 4a, 4b, 4c). We saw a slight bias in fluorescence intensity of calbindin away from the apical dendrite direction and near the PM; this trend was also seen in the analysis of another set of staining of calbindin (Fig. 2; Haberl et al., in preparation). Possible explanation for this slight bias could be that bulky organelles such as ER and mitochondria may have higher occupancies near the apical dendrite and towards the PM, causing Ca^{2+} buffers to have low distributions in these regions occupied by the organelles. This explanation is based on analyses of mitochondria import receptor subunit TOM20 located on mitochondrial membranes. TOM20 distribution shows clear bias towards the apical dendrite and the nuclear membrane, opposite to the bias observed for calbindin (Haberl et al., in preparation). In addition, the mitochondria have a higher density further away from the PM, based on the analysis of EM reconstruction (Haberl et al., in preparation). These two findings both suggested that the presence of bulky organelles might restrict Ca^{2+} buffer distributions in the same subcellular domains. Moreover, PMCA's significant preference towards the PM indicated that our IHC analysis can detect highly polarized protein fluorescence intensity as well. Overall, we are confident at some level that our IHC analysis can detect both wide and highly polarized distribution.

Not all Ca^{2+} signaling proteins in the GPCR-IP3R pathway have significant distribution patterns. PLCβs were expected to be localized to the PM, since they are closely associated with

$G_{\alpha q}$ subunits of GPCRs that are tightly attached to the PM (Fukaya et al., 2008; Scarlata et al., 2016). In our IHC, PLCβ1 does not indicate a high expression in the Purkinje soma, whereas its fluorescence is slightly higher in the apical dendrite (Fig. 3a). Moreover, PLCβ1 seems to have a preferential localization to the projections of PV basket cells to the axonal pole of Purkinje neurons (Fig. 3a, 3c). This observation agrees with previous IHC and immunogold electron microscopy analyses of PLCβ1; low levels of PLCβ1 fluorescence was observed in Purkinje somas, while PLCβ1 was more enriched in the pinceau formation, the clustered basket cell axons surrounding the initial Purkinje axons (Fukaya et al., 2008). Because of the low preference of PLCβ1 within Purkinje somas, PLCβ1 will not be further considered into the calcium diffusion model.

Different from PLCβ1, PLCβ3 is more expressed and widely distributed within the whole Purkinje neurons (Fig. 3b, 3e). This finding agrees with previous staining of PLCβ3 in cerebellum that PLCβ3 is highly expressed within Purkinje neurons (Nomura et al., 2007). Subcellular ultrastructure revealed preferential distribution of PLCβ3 around the spine membrane and smooth ER (Nomura et al., 2007). Upon closer examination of our PLCβ3 staining, PLCβ3 has slight drop-off of fluorescence intensity near the PM, but otherwise widely distributed within the Purkinje soma (Fig. 3e, 3f). Association with smooth ER could explain the high expression observed within the somatic space. In the same previous study, co-localizations between PLCβ3 and signaling proteins such as mGluR1, IP3R1 and scaffolding protein Homer1 could be observed in dendritic spines and shafts of Purkinje neurons, indicating important functional role of PLCβ3 in regulating Ca^{2+} diffusion between the PM and the ER (Nomura et al., 2007). However, possible explanation could not be ascertained for the slight bias against the PM, and further testing is needed to figure out why this decrease near the PM was observed. Nonetheless,

PLCβ3 is highly expressed and widely distributed in the whole Purkinje soma including the PM, and we will consider uniform distribution of PLCβ3 in the calcium diffusion model.

Although PLCβs do not have substantial heterogeneity within the Purkinje somas, IP3Rs were found to be heterogeneous within the somatic space (Haberl et al., in preparation). Although previous studies revealed heterogeneous localizations of Ca^{2+} stores across various cell compartments such as dendritic spines, dendritic shafts and soma bodies, the somatic spatial distribution of IP3Rs has not been studied extensively (Takei et al., 1992; Walton et al., 1991). The preference of IP3Rs towards the PM could be correlated to the higher densities of ERs near the PM, since IP3Rs are located on the PM (Fig. 1; Haberl et al., in preparation; Ross et al., 1989). Because IP3Rs are an important player in the GPCR-IP3R pathway that can amplify local Ca^{2+} diffusion, the unique distribution pattern of IP3Rs might indicate a distribution-function relationship (Lock et al., 2019; W. N. Ross, 2012). Further showing the importance of IP3R distribution in Ca^{2+} signaling dynamics, in the calcium diffusion model with idealized geometry, various densities of IP3Rs can induce different degrees of Ca^{2+} release from ER stores (Haberl et al., in preparation). This finding greatly supported our hypothesis that heterogeneous distributions of Ca^{2+} signaling molecules may shape Ca^{2+} signaling dynamics.

We could not observe any significant distribution patterns for mGluR1s, and therefore we will not change the uniform distribution pattern of mGluR1s in the calcium diffusion model. mGluR1s, as the initiator in the GPCR-IP3R pathway, are expected to be localized to the PM as they are transmembrane proteins active at the PM (Knöpfel & Grandes, 2002). Although the presence of mGluR1 could be detected within the Purkinje somatic space, it is very weak; mGluR1s fluorescence can be more prominently detected in the dendrites than in the somas (Fig. 4a). This preferential distribution of mGluR1s in the Purkinje dendrites and weaker but still present

distribution in the somatic space agree with previous studies that mGluR1s is more expressed in the Purkinje dendritic spines than perikarya (Baude et al., 1993; Nomura et al., 2007). As for the cytosolic mGluR1s, its presence could be explained by the detection of mGluR1s in the microsomal fractions of Purkinje neurons (Nakamura et al., 1999). Although our analysis of mGluR1s agrees with previous studies, we could not observe a significant distribution pattern of mGluR1s on the PM due to the permeabilization process during mGluR1s staining. As a result, we could not isolate the fluorescence of mGluR1s on the PM. Due to the low preference of mGluR1s towards the PM, we will not change the uniform distribution of mGluR1s in the model (Fig. 4d, 4g).

Neither 5HT2aRs nor M3 mAChRs has high expression within the Purkinje somas, and therefore we will not consider these alternative GPCRs in the calcium diffusion model. Both 5HT2aRs and M3 mAChRs are transmembrane proteins and thus are expected to localize to the PM (Caulfield, 1993). In our IHC analysis, 5HT2aR has a low to average expression within the Purkinje neuron, and has a preference towards the nuclear membrane with the somatic space (Fig. 4c, 4f, 4i). These findings match with previous experimental results where 5HT2aRs were moderately expressed within neuron cell bodies and has a higher distribution in the cytoplasm than on the plasma membrane (Cornea-Hébert et al., 1999). A possible explanation to these observations is that 5HT2aRs are mostly internalized during normal functions (Cornea-Hébert et al., 1999). Interestingly, a high expression of 5HT2aRs could be observed in the pinceau formation (basket cells projections onto Purkinje neurons) in the axonal pole of the Purkinje neuron, possibly indicating a functional distribution as a relation to the basket cell synaptic connections. As for M3 mAChRs, not much fluorescence was observed at all within the somatic space; within the somatic space, it has a preference towards the nuclear membrane (Fig. 4b, 4e, 4h). Not many studies have

focused on the subcellular distribution of M3 mAChRs, but one study has shown subcellular distribution pattern in M1 mAChRs, which also bind to G_q unit to activate PLCβ (Caulfield, 1993; Uwada et al., 2011). The M1 mAChRs were seen both on the PM and has a preference towards the nuclear membrane in the cytosol space. The author proposed a similar explanation for this intracellular observation: M1 mAChRs are either internalized or are newly synthesized in the ER and the golgi (Uwada et al., 2011). Overall, since we did not observe high expressions in the somatic space and both 5HT2aRs and M3 mAChRs do not seem to have preferences towards the PM, we will not consider these two GPCRs as possible alternatives to mGluR1.

In general, despite the fact that significant distribution patterns could not be observed for PLCβs and GPCRs except for IP3Rs, all distribution analyses are still very valuable because they presented subcellular spatial distributions of Ca^{2+} signaling proteins in the GPCR-IP3R pathway that have never been systemically studied before. Because of these analyses, we were able to decide whether or not to change the previously uniform distributions of these proteins in the Ca^{2+} diffusion model, and thus creating a realistic model that can predict precise Ca^{2+} signaling dynamics within the Purkinje somas. After the realistic Ca^{2+} diffusion model is generated based on all the analyses combined, we will have more insights into how subcellular ultrastructure and protein distributions can affect Ca^{2+} signaling dynamics. This model will prove to be a useful tool in investigating precise Ca^{2+} signaling dynamics in any cell, if ultrastructure organization and protein spatial distributions are gathered.

The next step we would like to see is the study of protein spatial distributions with super-resolution microscopy such as expansion microscopy. Because tissue samples can be expanded via attachment to swellable polyelectrolyte hydrogels, this imaging technique will allow a look with higher resolution (~4.5x) into the spatial distributions of Ca^{2+} signaling proteins under just light

microscopy (Wassie et al., 2019). Using this technique, we might be able to locate Ca^{2+}regulating proteins in certain subcellular domains and provide more detailed spatial information for the calcium diffusion model to be precise. Expansion microscopy might also be able to show co-localizations of proteins in the GPCR-IP3R pathway with higher magnitude of resolution, providing more spatial information about the functional distributions of these proteins within Purkinje somas, as studies have shown (but not quantified) or indicated co-localizations between PLCβ3 and mGluR1 or between IP3Rs, Homer1 (a scaffolding protein) and mGluRs (Berridge et al., 2003; Nomura et al., 2007). Therefore, expansion microscopy will be a valuable tool to investigate further into intracellular Ca^{2+} signaling dynamics.

MATERIALS AND METHODS

Animals

Male and female wild-type C57/BL6J (Jackson Laboratories) mice between 45-50 days postnatally were used for immunohistochemistry (IHC) experiments. A male C57BL/6NHsd mouse at day 40 postnatally was used for electron microscopy (EM) experiments. All experiments were approved by and performed according to a protocol provided by Institutional Animal Care and Use Committee (IACUC, protocol number S12254) of UC San Diego.

Tissue Preparation

In preparation of IHC experiments, C57/BL6J mice were anesthetized with 50-100 µL of ketamine via intraperitoneal injection. The mice were perfused with ddH_2O, phosphate-buffered saline (PBS) solution with heparin, and 4% paraformaldehyde (PFA) in PBS (diluted from 16% Paraformaldehyde aqueous solution (15710) by Electron Microscopy Sciences) at room temperature. Entire brains were extracted after perfusion and fixed in 4% PFA solution overnight at 4°C, followed by cryo-preservation in 30% sucrose solution for 1 to 2 days at 4°C. Sagittal cerebellar tissues of 50µm thickness were freeze-sectioned on a Leica microtome. Tissues on the Vermis region of cerebellum were selected for IHC and preserved in cryoprotectant solution at -20°C. Tissue preparation for electron microscopy (EM) experiments were performed by Matthias Haberl at the Ellisman Lab and was the same as described in Haberl et al. (2018).

3D reconstruction via electron microscopy

Volumetric images of cerebellar Purkinje neurons were acquired using serial block-face electron microscopy (SBEM) and electron tomography microscopy (ET). Methods for SBEM and ET experiments were as described in Haberl et al. (2018). Reconstructed resolution for SBEM and ET datasets were 4.2-6 nm voxelsize in x/y/z. A deep-learning image segmentation tool CDeep3M was employed to generate initial segmentations of Purkinje subcellular ultrastructure including endoplasmic reticulum, plasma membrane, nucleus, mitochondria and golgi apparatus, based on the SBEM dataset (Haberl et al. 2018). Annotations were manually corrected based on small EM datasets in IMOD software and the corrected annotations were subsequently used as training data for CDeep3M. Continuous training was performed to generate more and more predictions for ultrastructure segmentations for larger datasets (Haberl et al., 2018).

Immunohistochemistry (IHC)

Free floating cerebellar tissues were permeabilized in 1% Triton-X solution (diluted from 10% Triton-X solution by Sigma Aldrich 10789704001) in 1x PBS at room temperature for 10 minutes, and then were blocked in blocking buffer mix of 3% normal donkey serum (NDS) (Sigma Aldrich D9663), 1% bovine serum albumin (BSA) (diluted from 10% BSA), 1% cold water fish gelatin (diluted from 10% fish gelatin) and 0.1% Triton-X (diluted from 10% Triton-X by Sigma Aldrich 10789704001) in 1x PBS overnight at 4°C. Tissues were then incubated in primary antibodies (in a buffer mix of 10% of the blocking buffer and 0.1% Triton-X in 1x PBS), including 1/50 rabbit anti 5HT2aR polyclonal (Neuromics RA24288), 1/500 rabbit anti mGluR1 monoclonal

(Cell Signaling Technology 12551), 1/250 rabbit anti mAChR M3/CHRM3 polyclonal (Novus NLS5259), 1/100 rabbit anti parvalbumin polyclonal (Abcam ab11427), 1/100 rabbit anti PLCβ1 polyclonal (Proteintech 26551-1-AP), 1/100 mouse anti PLCβ3 monoclonal (Proteintech 66668-1-lg) and 1/800 guinea pig anti calbindin polyclonal (Synaptic Systems 214004), for 72 hours at 4°C. After primary antibody incubation, the tissues were incubated in secondary antibodies (in a working buffer mix as described above), including 1/500 donkey anti rabbit conjugated to Alexa 488 fluorophores, 1/500 donkey anti mouse conjugated to Alexa 488 fluorophores and 1/500 donkey anti guinea pig conjugated to Alexa 647 fluorophores, overnight for 24 hours at 4°C. Tissues were then stained with DAPI Fluoromount-G mounting media (SouthernBiotech 0100-20), mounted and sealed on glass slides.

Confocal Imaging and Analysis

Volumetric confocal images were acquired from stained cerebellar tissues at lobes IV, V and VI in the Vermis region of cerebellum, via Nikon A1 Confocal at 100x magnification at the Nikon Imaging Center at UC San Diego. The images are 116.24 μm in x/y and 0.175 μm in z. Conjugated fluorophores were excited at laser wavelengths of 403.7 nm (DAPI), 489.2 nm (FITCIx) and 640.2 nm (Cy5). Laser power and gain were set up to optimize signal to noise ratio. Confocal images were deconvolved using the Landweber algorithm in the NIS-Elements imaging software. Contour masks for Purkinje neurons were created based on calbindin staining, while contour masks for Purkinje nuclei were created based on DAPI staining in FIJI and IMOD software. Contour masks of Purkinje somas and apical dendrites were separated based on altering cell curvatures at the soma-dendrite boundaries. Eighteen Purkinje neurons were analyzed per

protein staining and 11-21 steps of images from the centers of the Purkinje neurons were chosen from each volumetric image to be analyzed in Matlab. In Matlab, the fluorescence intensity of each protein only in the cytosol space was analyzed based on the contour masks via scripts created by Evan Campbell. The fluorescence intensities were analyzed angularly, by dividing the cytosol spaces into twelve 30-degree sub-regions based on a polar coordinate centered on the neuronal center. The fluorescence intensities were also analyzed radially from the nuclear membrane boundary to the plasma membrane boundary. One-way ANOVAS were performed to produce the p-values for each analysis in Prism GraphPad.

Calcium Diffusion Model

The Calcium diffusion model with idealized geometry was constructed using partial differential equations by Justin Laughlin at Rangamani Lab, UC San Diego. The model inputted calcium and IP3 diffusion dynamics based on previous experiments.

Acknowledgment

This thesis, in part, is currently being prepared for submission for publication of the material. Co-authors of the publication in preparation include Matthias G. Haberl, Justin Laughlin, Evan P. Campbell, Kaitlyn Robinson, Lukas Makrakis, Andrew Nguyen, Justin Oshiro, Sebastien Phan, Eric Bushong, Thomas Deerinck, Mark H. Ellisman, Padmini Rangamani and Brenda L Bloodgood. The thesis author was the primary investigator and author of this material.

REFERENCES

Allbritton, N. L., Meyer, T., & Stryer, L. (1992). Range of messenger action of calcium ion and inositol 1,4,5-trisphosphate. *Science*, *258*(5089), 1812–1815. https://doi.org/10.1126/science.1465619

Apps, R., & Garwicz, M. (2005). Anatomical and physiological foundations of cerebellar information processing. *Nature Reviews Neuroscience*, *6*(4), 297–311. https://doi.org/10.1038/nrn1646

Azmitia, E. C. (2001). Modern views on an ancient chemical: Serotonin effects on cell proliferation, maturation, and apoptosis. *Brain Research Bulletin*, *56*(5), 413–424. https://doi.org/10.1016/S0361-9230(01)00614-1

Baude, A., Nusser, Z., Roberts, J. D. B., Mulvihill, E., Mcllhinney, R. A. J., & Somogyi, P. (1993). The Metabotropic Glutamate Receptor (mGluRla) Is Concentrated at Perisynaptic Membrane of Neuronal Subpopulations as Dekckd by lmmunogold Reaction. *Neuron*, *11*, 771–787.

Berridge, M. J. (1998). Neuronal Calcium Signaling. *Neuron*, *21*, 13–26.

Berridge, M. J., Bootman, M. D., & Roderick, H. L. (2003). Calcium Signalling: Dynamics, Homeostasis and Remodelling. *Nature Reviews*, *4*(July). https://doi.org/10.1038/nrm1155

Berridge, M. J., Lipp, P., & Bootman, M. D. (2000). The Versatility and Universatility of Calcium Signalling. *Nature Reviews*, *1*(October), 11–21.

Blaustein, M. P., & Golovina, V. A. (2001). Structural complexity and functional diversity of endoplasmic reticulum Ca2+ stores. *Trends in Neurosciences*, *24*(10), 602–608. https://doi.org/10.1016/S0166-2236(00)01891-9

Bloodgood, B. L., & Sabatini, B. L. (2007). Ca2+ signaling in dendritic spines. *Current Opinion in Neurobiology*, *17*(3), 345–351. https://doi.org/10.1016/j.conb.2007.04.003

Bootman, M. D., Berridge, M. J., & Lipp, P. (1997). Cooking with calcium: The recipes for composing global signals from elementary events. *Cell*, *91*(3), 367–373. https://doi.org/10.1016/S0092-8674(00)80420-1

Calì, T., Brini, M., & Carafoli, E. (2018). The PMCA pumps in genetically determined neuronal pathologies. *Neuroscience Letters*, *663*(September 2017), 2–11. https://doi.org/10.1016/j.neulet.2017.11.005

Caulfield, M. P. (1993). Muscarinic Receptors-Characterization, coupling and function. *Pharmacology and Therapeutics*, *58*(3), 319–379. https://doi.org/10.1016/0163-7258(93)90027-B

Chemaly, E. R., Troncone, L., & Lebeche, D. (2018). SERCA Control of Cell Death and Survival. *Cell Calcium*, *69*, 46–61. https://doi.org/10.1016/j.ceca.2017.07.001.SERCA

Citri, A., & Malenka, R. C. (2008). Synaptic Plasticity : Multiple Forms, Functions, and Mechanisms. *Neuropsychopharmacology*, *33*, 18–41. https://doi.org/10.1038/sj.npp.1301559

Collins, T. J., Lipp, P., Berridge, M. J., & Bootman, M. D. (2001). Mitochondrial Ca2+ Uptake Depends on the Spatial and Temporal Profile of Cytosolic Ca2+ Signals. *Journal of Biological Chemistry*,

276(28), 26411–26420. https://doi.org/10.1074/jbc.M101101200

Cornea-Hébert, V., Riad, M., Wu, C., Singh, S. K., & Descarries, L. (1999). Cellular and Subcellular Distribution of the Serotonin 5-HT2A Receptor in the Central Nervous System of Adult Rat. *The Journal of Comparative Neurology*, *409*, 187–209.

Cresswell-clay, E., Crock, N., Tabak, J., & Erlebacher, G. (2018). A Compartmental Model to Investigate Local and Global Ca 2 + Dynamics in Astrocytes. *Frontiers in Computational Neuroscience*, *12*(94), 1–14. https://doi.org/10.3389/fncom.2018.00094

Dhyani, V., Gare, S., Gupta, R. K., Swain, S., Venkatesh, K. V, & Giri, L. (2020). GPCR mediated control of calcium dynamics : A systems perspective. *Cellular Signaling*, *74*(January).

Dickinson, G. D., Ellefsen, K. L., Dawson, S. P., Pearson, J. E., & Parker, I. (2017). Hindered cytoplsmic diffusion of inositol trisphosphate restricts its cellular range of action. *Sci Signal.*, *9*(453). https://doi.org/10.1016/j.physbeh.2017.03.040

Empson, R. M., & Knöpfel, T. (2012). Functional integration of calcium regulatory mechanisms at purkinje neuron synapses. *Cerebellum*, *11*(3), 640–650. https://doi.org/10.1007/s12311-010-0185-6

Fierro, L., & Llano, I. (1996). High endogenous calcium buffering in Purkinje cells from rat cerebellar slices. *Journal of Physiology*, *496*(3), 617–625.

Finch, E. A., & Augustine, G. J. (1998). Local calcium signalling by inositol-1,4,5-trisphosphate in Purkinje cell dendrites. *Nature*, *396*, 753–756.

Fink, C. C., Slepchenko, B., Moraru, I. I., Watras, J., Schaff, J. C., & Loew, L. M. (2000). An Image-Based Model of Calcium Waves in Differentiated Neuroblastoma Cells. *Biophysical Journal*, *79*, 163–183.

Foster, T. C., & Norris, C. M. (1997). Age-Associated Changes in Ca2+-Dependent Processes: Relation to Hippocampal Synaptic Plasticity. *Hippocampus*, *7*, 602–612.

Foster, T. C., Sharrow, K. M., Masse, J. R., Norris, C. M., & Kumar, A. (2001). Calcineurin Links Ca2+ Dysregulation with Brain Aging. *The Journal of Neuroscience*, *21*(11), 4066–4073.

Fukaya, M., Uchigashima, M., Nomura, S., Hasegawa, Y., Kikuchi, H., & Watanabe, M. (2008). Predominant expression of phospholipase C b 1 in telencephalic principal neurons and cerebellar interneurons , and its close association with related signaling molecules in somatodendritic neuronal elements. *European Journal of Neuroscience*, *28*, 1744–1759. https://doi.org/10.1111/j.1460-9568.2008.06495.x

Gilabert, J. A. (2020). Cytoplasmic Calcium Buffering : An Integrative Crosstalk. *Calcium Signaling, Advances in Experimental Medicine and Biology*, *1131*, 163–182.

Grewal, S. S., Horgan, A. M., York, R. D., Withers, G. S., Banker, G. A., & Stork, P. J. S. (2000). Neuronal Calcium Activates a Rap1 and B-Raf Signaling Pathway via the Cyclic Adenosine Monophosphate-dependent Protein Kinase. *Journal of Biological Chemistry*, *275*(5), 3722–3728. https://doi.org/10.1074/jbc.275.5.3722

Gruol, D., Manto, M., & Haines, D. (2012). Ca2+ Signaling in Cerebellar Purkinje Neurons -

EDITORIAL. *Cerebellum*, *1*(2), 605–608. https://doi.org/10.1007/s12311-012-0404-4.Ca

Haberl, M. G., Churas, C., Tindall, L., Boassa, D., Phan, S., Bushong, E. A., Madany, M., Akay, R., Deerinck, T. J., Peltier, S. T., & Ellisman, M. H. (2018). CDeep3M — Plug-and-Play cloud-based deep learning for image segmentation. *Nature Methods*, *15*, 677–680. https://doi.org/10.1038/s41592-018-0106-z

Hagenston, A. M., & Simonetti, M. (2014). Neuronal calcium signaling in chronic pain. *Cell Tissue Res*, *357*, 407–426. https://doi.org/10.1007/s00441-014-1942-5

Hardingham, G. E., Chawla, S., Johnson, C. M., & Bading, H. (1997). Distinct functions of nuclear and cytoplasmic calcium in the control of gene expression. *Nature*, *385*(6613), 260–265. https://doi.org/10.1038/385260a0

Hartmann, J., & Konnerth, A. (2005). Determinants of postsynaptic Ca2+ signaling in Purkinje neurons. *Cell Calcium*, *37*(5 SPEC. ISS.), 459–466. https://doi.org/10.1016/j.ceca.2005.01.014

Hayer, S. N., & Bading, H. (2015). Nuclear Calcium Signaling Induces Expression of the Synaptic Organizers Lrrtm1 and Lrrtm2. *The Journal of Biological Chemistry*, *290*(9), 5523–5532. https://doi.org/10.1074/jbc.M113.532010

Hoxha, E., Tempia, F., Lippiello, P., & Miniaci, M. C. (2016). Modulation, plasticity and pathophysiology of the parallel fiber-purkinje cell synapse. *Frontiers in Synaptic Neuroscience*, *8*(November), 1–16. https://doi.org/10.3389/fnsyn.2016.00035

Ito, M. (2002). Historical Review of the Significance of the Cerebellum and the Role of Purkinje Cells in Motor Learning. *Ann. N.Y. Acad. Sci.*, *978*, 273–288.

Kadamur, G., & Ross, E. M. (2013). Mammalian Phospholipase C. *Annual Review of Physiology*, *75*(1), 127–154. https://doi.org/10.1146/annurev-physiol-030212-183750

Knöpfel, T., & Grandes, P. (2002). Metabotropic glutamate receptors in the cerebellum with a focus on their function in Purkinje cells. *Cerebellum*, *1*(1), 19–26. https://doi.org/10.1080/147342202753203050

Krebs, J., Agellon, L. B., & Michalak, M. (2015). Biochemical and Biophysical Research Communications Ca2+ homeostasis and endoplasmic reticulum (ER) stress : An integrated view of calcium signaling. *Biochemical and Biophysical Research Communications*, *460*(1), 114–121. https://doi.org/10.1016/j.bbrc.2015.02.004

Kruse, A. C., Hu, J., Pan, A. C., Arlow, D. H., Rosenbaum, D. M., Rosemond, E., Green, H. F., Liu, T., Chae, P. S., Dror, R. O., David, E., Weis, W. I., Wess, J., & Kobilka, B. (2012). Structure and Dynamics of the M3 Muscarinic Acetylcholine Receptor. *Nature*, *482*(7386), 552–556. https://doi.org/10.1038/nature10867.Structure

Lock, J. T., Smith, I. F., & Parker, I. (2019). Spatial-temporal patterning of Ca2+ signals by the subcellular distribution of IP3 and IP3 receptors. *Semin Cell Dev Biol.*, *94*, 3–10. https://doi.org/10.1016/j.semcdb.2019.01.012.Spatial-temporal

Maskey, D., Pradhan, J., Kim, H., Park, K. S., Ahn, S. C., & Kim, M. J. (2010). Neuroscience Letters Immunohistochemical localization of calbindin D28-k , parvalbumin , and calretinin in the

cerebellar cortex of the circling mouse. *Neuroscience Letters*, *483*(2), 132–136. https://doi.org/10.1016/j.neulet.2010.07.077

Matthews, E. A., & Dietrich, D. (2015). Buffer mobility and the regulation of neuronal calcium domains. *Frontiers in Cellular Neuroscience*, *9*(February), 1–11. https://doi.org/10.3389/fncel.2015.00048

Moccia, F., Zuccolo, E., Soda, T., Tanzi, F., Guerra, G., Mapelli, L., Lodola, F., & D'Angelo, E. (2015). Stim and Orai proteins in neuronal Ca 2 + signaling and excitability. *Frontiers in Cellular Neuroscience*, *9*(April), 1–14. https://doi.org/10.3389/fncel.2015.00153

Nabavi, S., Fox, R., Proulx, C. D., Lin, J. Y., Tsien, R. Y., & Malinow, R. (2014). Engineering a memory with LTD and LTP. *Nature*, *511*(7509), 348–352. https://doi.org/10.1038/nature13294

Nakamura, T., Barbara, J.-G., Nakamura, K., & Ross, W. N. (1999). Synergistic Release of Ca 2 ⁺ from IP 3 -Sensitive Stores Evoked by Synaptic Activation of mGluRs Paired with Backpropagating Action Potentials. *Neuron*, *24*, 727–737.

Neher, B. Y. E., & Augustine, G. J. (1992). CALCIUM GRADIENTS AND BUFFERS IN BOVINE CHROMAFFIN Cells. *Journal of Physiology*, *450*, 273–301.

Nixon-Abell, J., Obara, C. J., Weigel, A. V., Li, D., Legant, W. R., Xu, C. S., Pasolli, H. A., Harvey, K., Hess, H. F., Betzig, E., Blackstone, C., & Lippincott-Schwartz, J. (2016). Increased spatiotemporal resolution reveals highly dynamic dense tubular matrices in the peripheral ER. *Science*, *354*(6311). https://doi.org/10.1126/science.aaf3928

Nomura, S., Fukaya, M., Tsujioka, T., Wu, D., & Watanabe, M. (2007). Phospholipase Cβ3 is distributed in both somatodendritic and axonal compartments and localized around perisynapse and smooth endoplasmic reticulum in mouse Purkinje cell subsets. *European Journal of Neuroscience*, *25*(3), 659–672. https://doi.org/10.1111/j.1460-9568.2007.05334.x

Orrenius, S., Zhivotovsky, B., & Nicotera, P. (2003). REGULATION OF CELL DEATH : THE CALCIUM – APOPTOSIS LINK. *Nature Reviews*, *4*(July), 552–565. https://doi.org/10.1038/nrm1150

Power, J. M., & Sah, P. (2002). Nuclear Calcium Signaling Evoked by Cholinergic Stimulation in Hippocampal CA1 Pyramidal Neurons. *The Journal of Neuroscience*, *22*(9), 3454–3462.

Rhee, S. G. (2001). R Egulation of P Hosphoinositide -S Pecific. *Annu. Rev. Biochem*, *70*, 281–312.

Ross, C. A., Meldolesit, J., Milner, T. A., Satoht, T., Supattapone, S., & Snyder, S. H. (1989). Inositol 1, 4, 5-triphosphate receptor localized to endoplasmic reticulum in cerebellar Purkinje neurons. *Nature*, *339*(June), 468–470.

Ross, W. N. (2012). Understanding calcium waves and sparks in central neurons. *Nature Reviews Neuroscience*, *13*(3), 157–168. https://doi.org/10.1038/nrn3168

Satoh, T., Ross, C. A., Villa, A., Supattapone, S., Pozzan, T., Snyder, S. H., & Meldolesi, J. (1990). The inositol 1,4,5,-trisphosphate receptor in cerebellar Purkinje cells: Quantitative immunogold labeling reveals concentration in an ER subcompartment. *Journal of Cell Biology*, *111*(2), 615–624. https://doi.org/10.1083/jcb.111.2.615

Scarlata, S., Garwain, O., Williams, L., Burguera, I. G., Rosati, B., Sahu, S., Guo, Y., Philip, F., & Golebiewska, U. (2016). PHOSPHOLIPASE Cβ CONNECTS G PROTEIN SIGNALING WITH RNA INTERFERENCE. *Adv Biol Regul.*, *61*, 51–57. https://doi.org/10.1016/j.jbior.2015.11.006.PHOSPHOLIPASE

Schwaller, B. (2010). Cytosolic Ca2+ Buffers. *Cold Spring Harbor Perspectives in Biology*, 1–20.

Silva, A. J., Kogan, J. H., Frankland, P. W., & Kida, S. (1998). Creb and memory. *Annu. Rev. Neurosci.*, *21*, 127–148.

Stefan, C. J., Manford, A. G., & Emr, S. D. (2013). ER–PM connections: sites of information transfer and inter- organelle communication. *Curr Opin Cell Biol*, *25*(4), 434–442. https://doi.org/10.1016/j.ceb.2013.02.020.ER

Swillens, S., Dupont, G., Combettes, L., & Champeil, P. (1999). From calcium blips to calcium puffs: Theoretical analysis of the requirements for interchannel communication. *Proceedings of the National Academy of Sciences of the United States of America*, *96*(24), 13750–13755. https://doi.org/10.1073/pnas.96.24.13750

Takei, K., Stukenbrok, H., Metcalf, A., Mignery, G. A., Siidhof, T. C., Volpe, P., & Camilw, P. De. (1992). Ca 2+ Stores in Purkinje Neurons : Endoplasmic Reticulum Subcompartments Demonstrated by the Heterogeneous Distribution of the InsP3, Receptor, Ca2+ -ATPase , and Calsequestrin. *The Journal of Neuroscience*, *12*(2), 489–505.

Talamoni, N. T. de, Smith, C. A., Wasserman, R. H., Beltramino, C., Fullmer, C. S., & Penniston, J. T. (1993). Immunocytochemical localization of the plasma membrane calcium pump , calbindin-D28k , and parvalbumin in Purkinje cells of avian and mammalian cerebellum. *Proc. Natl. Acad. Sci.*, *90*, 11949–11953.

Tao-Cheng, & Jung-Hwa. (2018). Activity-dependent decrease in contact areas between subsurface cisterns and plasma membrane of hippocampal neurons. *Molecular Brain*, *11*(23), 1–8.

Taylor, C. W., Taufiq-Ur-Rahman, & Pantazaka, E. (2009). Targeting and clustering of IP3 receptors: Key determinants of spatially organized Ca2+ signals. *Chaos*, *19*(3). https://doi.org/10.1063/1.3127593

Terasaki, M., Slater, N. T., Fein, A., Schmidek, A., & Reese, T. S. (1994). Continuous network of endoplasmic reticulum in cerebellar Purkinje neurons. *Proceedings of the National Academy of Sciences of the United States of America*, *91*(16), 7510–7514. https://doi.org/10.1073/pnas.91.16.7510

Thillaiappan, N. B., Chavda, A. P., Tovey, S. C., Prole, D. L., & Taylor, C. W. (2017). Ca2+ signals initiate at immobile IP3 receptors adjacent to ER-plasma membrane junctions. *Nature Communications*, *8*(1). https://doi.org/10.1038/s41467-017-01644-8

Uwada, J., Anisuzzaman, A. S. M., Nishimune, A., Yoshiki, H., & Muramatsu, I. (2011). Intracellular distribution of functional M1-muscarinic acetylcholine receptors in N1E-115 neuroblatoma cells. *Journal of Neurochemistry*, *118*, 958–967. https://doi.org/10.1111/j.1471-4159.2011.07378.x

Walton, P. D., Airey, J. A., Sutko, J. L., Beck, C. E., Mignery, G. A., Südhof, T. C., Deerinck, T. J., & Ellisman, M. H. (1991). Ryanodine and Inositol Trisphosphate Receptors Coexist in Avian

Cerebellar Purkinje Neurons. *The Journal of Cell Biology*, *113*(5), 1145–1157.

Wassie, A. T., Zhao, Y., & Boyden, E. S. (2019). Expansion microscopy: principles and uses in biological research. *Nature Methods*, *16*(1), 33–41. https://doi.org/10.1038/s41592-018-0219-4

Wei, P., Blundon, J. A., Rong, Y., Zakharenko, S. S., & Morgan, J. I. (2011). Impaired Locomotor Learning and Altered Cerebellar Synaptic Plasticity in pep-19/pcp4-Null Mice. *Molecular and Cellular Biology*, *31*(14), 2838–2844. https://doi.org/10.1128/mcb.05208-11

Wiegert, J. S., & Bading, H. (2011). Cell Calcium Activity-dependent calcium signaling and ERK-MAP kinases in neurons : A link to structural plasticity of the nucleus and gene transcription regulation. *Cell Calcium*, *49*(5), 296–305. https://doi.org/10.1016/j.ceca.2010.11.009

Wu, M. M., Buchanan, J., Luik, R. M., & Lewis, R. S. (2006). Ca2+ store depletion causes STIM1 to accumulate in ER regions closely associated with the plasma mebrane. *Journal of Cell Biology*, *174*(6), 803–813. https://doi.org/10.1083/jcb.200604014

Wu, Y., Whiteus, C., Xu, C. S., Hayworth, K. J., Weinberg, R. J., Hess, H. F., & De Camilli, P. (2017). Contacts between the endoplasmic reticulum and other membranes in neurons. *Proceedings of the National Academy of Sciences of the United States of America*, *114*(24), E4859–E4867. https://doi.org/10.1073/pnas.1701078114